Neurobiology of Disease

Alzheimer's Disease: Presenilin 2-Sparing γ-Secretase Inhibition Is a Tolerable Aβ Peptide-Lowering Strategy

Tomas Borgegård,[1]* Susanne Gustavsson,[1]* Charlotte Nilsson,[1]* Santiago Parpal,[1]* Rebecka Klintenberg,[1]* Anna-Lena Berg,[1]* Susanne Rosqvist,[1] Lutgarde Serneels,[2,3] Samuel Svensson,[1,8,9] Fredrik Olsson,[1] Shaobo Jin,[4] Hongmei Yan,[1] Johanna Wanngren,[5] Anders Jureus,[1] Anna Ridderstad-Wollberg,[1] Patrik Wollberg,[1] Kenneth Stockling,[1] Helena Karlström,[5] Åsa Malmberg,[1] Johan Lund,[1] Per I. Arvidsson,[1,6,7] Bart De Strooper,[2,3] Urban Lendahl,[4] and Johan Lundkvist[1,5,9]

[1]AstraZeneca, CNS and Pain Innovative Medicines, SE-15185 Södertälje, Sweden, [2]Center for Human Genetics and Leuven Institute for Neurodegenerative Disorders (LIND), University of Leuven, 3000 Leuven Belgium, [3]VIB Center for the Biology of Disease (VIB11), 3000 Leuven, Belgium, [4]Department of Cell and Molecular Biology, Karolinska Institute, SE-171 77 Stockholm, Sweden, [5]Department of Neurobiology, Caring Sciences and Society, KI-Alzheimer Disease Research Center, Karolinska Institutet, Novum, SE-141 86 Stockholm, Sweden, [6]Organic Pharmaceutical Chemistry, Department of Medicinal Chemistry, Uppsala Biomedical Centre, Uppsala University, SE-751 23 Uppsala, Sweden, [7]School of Pharmacy and Pharmacology, Westville Campus, University of KwaZulu-Natal, Durban 4000, South Africa, [8]Department of Pharmacology, Linköping University, Sweden, and [9]Alzacure Foundation, Korphoppsgatan 33, SE-12064 Stockholm, Sweden

γ-Secretase inhibition represents a major therapeutic strategy for lowering amyloid β (Aβ) peptide production in Alzheimer's disease (AD). Progress toward clinical use of γ-secretase inhibitors has, however, been hampered due to mechanism-based adverse events, primarily related to impairment of Notch signaling. The γ-secretase inhibitor MRK-560 represents an exception as it is largely tolerable *in vivo* despite displaying only a small selectivity between Aβ production and Notch signaling *in vitro*. In exploring the molecular basis for the observed tolerability, we show that MRK-560 displays a strong preference for the presenilin 1 (PS1) over PS2 subclass of γ-secretases and is tolerable in wild-type mice but causes dose-dependent Notch-related side effect in PS2-deficient mice at drug exposure levels resulting in a substantial decrease in brain Aβ levels. This demonstrates that PS2 plays an important role in mediating essential Notch signaling in several peripheral organs during pharmacological inhibition of PS1 and provide preclinical *in vivo* proof of concept for PS2-sparing inhibition as a novel, tolerable and efficacious γ-secretase targeting strategy for AD.

Introduction

Alzheimer's disease (AD) is a devastating neurodegenerative disorder, which lacks disease modifying therapy. In AD the Amyloid β peptide (Aβ), which is generated from the processing of amyloid precursor protein (APP) by the enzyme γ-secretase, aggregates to form neural plaques, which induces a cascade of events resulting in neuronal loss and dementia (Karran et al., 2011). γ-Secretase is composed of four proteins, Presenilin 1 (PS1) or PS2, nicastrin, Pen-2, and Aph-1α or β (Steiner et al., 2008). The PS proteins constitute the enzymatic moiety of γ-secretase and are the molecular targets of established classes of γ-secretase inhibitors (GSIs) (De Strooper et al., 1998; Morohashi et al., 2006). A spectrum of GSIs has been developed (Imbimbo et al., 2011), but progress toward clinical use has been hampered by the fact that γ-secretase cleaves not only APP, but a large number of other transmembrane proteins (Haapasalo and Kovacs, 2011), most notably the Notch receptors (De Strooper et al., 1999; Milano et al., 2004).

To potentially circumvent the problems encountered in the clinical trials, it is important to explore the potential of γ-secretase subcomplex-specific inhibitors as a novel strategy to produce more tolerable GSIs (Serneels et al., 2009). Gene targeting of γ-secretase subunits in mice has revealed distinct physiological roles for specific γ-secretase components *in vivo* (Saura et al., 2004; Serneels et al., 2005). In the context of AD, it is of particular interest that PS1 seems to catalyze the vast majority of CNS Aβ production (De Strooper et al., 1998; Borgegard et al., 2011) and that certain GSIs of the sulfonamide class appear to exhibit a preference for PS1 over PS2 γ-secretase activities (Zhao et al., 2008; Borgegard et al., 2011), supporting the notion that development of γ-secretase subcomplex selective GSIs may be feasible. In line with this, the sulfonamide GSI, MRK-560, inhibits Aβ production in an efficacious manner and reduces neural plaque formation without producing the Notch-related off target effects observed in chronic studies in mice (Best et al., 2007). The mechanism by which Notch signaling is spared using MRK-560 has, however, not been unraveled, but

Received March 24, 2012; revised Aug. 29, 2012; accepted Sept. 18, 2012.

Author contributions: T.B., S.G., C.N., S.P., R.K., S.S., A.R.-W., J. Lund, P.I.A., U.L., and J. Lundkvist designed research; T.B., S.G., S.P., R.K., A.-L.B., S.R., L.S., S.S., F.O., S.J., H.Y., A.J., A.R.-W., P.W., and K.S. performed research; L.S., S.J., J.W., P.W., H.K., and B.D.S. contributed unpublished reagents/analytic tools; T.B., S.G., C.N., S.P., R.K., A.-L.B., S.R., L.S., F.O., S.J., H.Y., A.J., A.R.-W., K.S., A.M., P.I.A., B.D.S., U.L., and J. Lundkvist analyzed data; S.P., A.-L.B., S.S., U.L., and J. Lundkvist wrote the paper.

This work was financially supported by the Swedish Cancer Society; the Swedish Research Council (DBRM and Project Grant); the EC project NotchIT, Karolinska Institutet; and the VINNOVA Grant AZ-KI Gene and a Methusalem Grant (Flanders and KU Leuven) to B.D.S. We are grateful to Susanne Bergstedt for technical assistance and Gang Liu for HEK/APP cell line.

*T.B., S.G., C.N., S.P., R.K., and A.-L.B. contributed equally to this work.

The authors declare no competing financial interests.

Correspondence should be addressed to either of the following: Johan Lundkvist, Alzacure Foundation, Korhoppsgatan 33, SE 12064 Stockholm, Sweden, E-mail: lunkan@alzacure.org, or Urban Lendahl, Department of Cell and Molecular Biology, Karolinska Institute, SE-171 77 Stockholm, Sweden, E-mail: urban.lendahl@ki.se.

DOI:10.1523/JNEUROSCI.1451-12.2012

 0270-6474/12/3217297-09$15.00/0

is important to elucidate, as such information may guide development of the next generation GSIs.

In this study, we explore the differential effects of MRK-560 on APP and Notch processing. We find that while MRK-560 can inhibit cleavage of both APP and Notch with similar potency in cell lines, it acts differently on PS1- or PS2-containing γ-secretases: MRK-560 interacts differently with and more potently inhibits its PS1-containing γ-secretase. MRK-560 treatment of mice genetically deficient for PS2 resulted in Notch-related toxicity, whereas no toxicity was seen in wild-type (WT) mice. This combination of selectivity for PS1 and increased sensitivity for Notch-related toxicity in PS2-deficient mice demonstrates that PS2 carries out an important part of Notch processing in peripheral organs during pharmacological inhibition of PS1, and explains why Notch is spared after long term use of MRK-560.

Materials and Methods

Compounds. (*S*,*S*)-2-[2-(3,5-difluorophenyl)acetylamino]-*N*-(5-methyl-6-oxo-6,7-dihydro-5*H*-dibenzo[*b*,*d*]azepin-7-yl)propionamide, Dibenzazepine (DBZ), was purchased from Calbiochem (cat #565789). Tritium labeling of DBZ has been previously described (Malmquist et al., 2012). MRK-560 was synthesized according to a published method (Churcher et al., 2006).

Aβ measurement in cell culture experiments. HEK293 cells stably expressing human APP (HEK/APP), PS1 (HEK_PS1), and PS2 (HEK_PS2) have been described previously (Strömberg et al., 2005). Blastocyst-derived mouse cells (BD8) genetically ablated for both PS1 and PS2 were stably transfected with an hAPP695 encoding plasmid. HEK_PS cells were transiently transfected with C99 cDNA and BD8/APP cells with either mouse PS1 or mouse PS2 cDNAs, 24 h before compound exposure. Cells were cultured in 96- or 384-well plates and drugs were added to the cells in prewarmed fresh medium. Conditioned medium was harvested 5 h later and Aβ peptides were recorded using the Mesoscale discovery platform according to the manufacturer's description. Human and mouse Aβ peptides were analyzed using 6E10 and 4G8 antibodies, respectively, and specific C-terminal antibodies for x-37, x-38, x-39, x-40, and x-42 as described previously (Borgegard et al., 2012).

Analysis of γ-secretase-dependent APP intracellular domain release (luciferase reporter assay). The assay was performed essentially as described previously (Karlström et al., 2002). Briefly, HEK_PS1 and HEK_PS2 cells were transiently transfected using 75 ng MH100, 50 ng CMV-β-gal, and 75 ng C99-GVP in 96-well tissue culture plates, allowing quadruplicates within each experiment. Cells were then exposed to compound for 16 h before being washed and lysed using 100 μl cell lysis buffer per well (10 mM Tris pH 8.1, 1 mM EDTA, 150 mM NaCl, and 0.65% Nonidet P-40), and luciferase activity was monitored luminometrically after addition of luciferin and ATP (BioThema AB). To adjust for differences in transfection efficiencies, the β-gal activity of the cell lysate was determined by measuring absorbance at 405 nm in β-gal buffer (10 nM KCl, 60 mM Na_2HPO_4, 40 mM NaH_2PO_4, 1 mM MgCl2, 50 μM β-mercaptoethanol, and 8 mM *O*-nitrophenyl-β-D-galactopyranoside).

Analysis of γ-secretase-dependent Notch activation. The assay was performed essentially as described previously (Borgegard et al., 2012). Briefly HEK_PS1 and HEK_PS2 cells (Strömberg et al., 2005) were treated with 1 μg/ml doxycycline for 48 h before transient transfection with the extracellular truncated Notch (Notch1ΔE). Ten thousand cells per well were plated in 384 poly-D-lysine-coated wells and exposed to different concentrations of compounds for 12 h. Cells were then washed in PBS followed by fixation in 4% paraformaldehyde followed by immune staining with the anti-Val1744 antibody (Cell Signaling Technology), which specifically detects the N-terminal valine of γ-secretase-liberated Notch1 intracellular domain (NICD) and a secondary fluorescent-labeled antibody (Alexa Fluor 594; Invitrogen). Images were captured using the ImageXpress scanner (Molecular Devices) and automatic fluorescence measurements were performed using an algorithm for the average fluorescence in the nucleus under different conditions and compared relative to. 0.5% dimethylsulfoxide (DMSO; 100% control) and 500 nM L685458 (0% control). Each concentration was tested in duplicate in at least two separate experiments.

Membrane competition binding studies. Binding studies were performed in membranes prepared from either HEK_PS1 or HEK_PS2 (see above) overexpressing cells. Cells were induced with 1 μg/ml doxycycline for 48 h before harvesting in cold PBS. After washing, cells were homogenized in ice-cold buffer (10 mM Tris, pH7.4, 5 mM EDTA supplemented with 0.1% w/v bacitracin) with 10 strokes on a Teflon Potter Homogenizer, and then centrifuged at 48,000 × *g* for 30 min. Pellets were washed once with 10 mM Tris, pH7.4, 5 mM EDTA, centrifuged as above, and resuspended in the same buffer before storage at −80°C. Membranes (40 μg protein/point), and increasing amounts of either cold DBZ or MRK-560 were diluted in binding buffer (50 mM MES, 100 mM NaCl, 1 mM EDTA, pH 6.5) and mixed together. After 1 h incubation, [^{3}H]-DBZ (specific activity 90 μM, at 0.95–2.6 nM final concentration) was added to a final volume of 500 μl. After 2 h, the samples were filtrated and washed and the radioactivity bound detected with the help of a Liquid Scintillation Analyzer (Packard).

Mouse brain autoradiography. In vitro autoradiography was performed on 10 μm frozen rat brain sections cut through the sagittal plane on a cryostate. The sections were thaw mounted onto microscope slides (SuperFrost Plus slides; Menzel GmBh), air dried, and stored at −80°C until used. Before binding experiments sections were warmed to room temperature and preincubated for 10 min at room temperature in 50 mM Tris-buffer, pH 7.4, then transferred to the same buffer containing 1–10 nM [^{3}H]DBZ and incubated for 45 min at room temperature. The sections were then washed sequentially 3 × 7 min in ice-cold buffer to remove excess unlabeled radio tracer, dipped in ice-cold distilled water, and finally air dried in front of a fan. For competition studies, adjacent tissue sections were incubated in the same buffer with radiotracers but in the presence of different concentrations of unlabeled DBZ or MRK-560. Radio-labeled sections and plastic tritium standards (GE Healthcare Bioscience) were exposed to imaging plates (Fuji BAS-TR2040; Fuji Photo Film) for 5 d. The Imaging plates were processed with a FLA7000 Imaging Reader (Fujifilm). Binding was analyzed with Multigauge software V3.0 (Fujifilm).

Thymus, spleen, and brain radio-ligand binding analysis. [^{3}H]DBZ (0.56 TBq/mmol, radiochemical purity >99%) was prepared following a previously published method (Malmquist et al., 2012). [^{3}H]DBZ binding assays on crude plasma membrane fraction prepared from frozen spleen, thymus, or brain were performed in a volume of 500 μl binding buffer (25 mM Tris-HCl, pH7.4, 50 mM NaCl, 0.5 mM EDTA) containing plasma membrane (0.1–1 μg/ml), 0.5 nM [^{3}H]DBZ, and 1 μM semagacestat or DMSO. The samples were incubated for 1 h at 22°C. Nonspecific, nondisplaceable binding was defined in the presence of 1 μM semagacestat diluted in DMSO. The incubation was terminated by filtration through Whatman GF/B glass microfiber filter (Whatman), and washed rapidly four times with 2 ml of ice-cold wash buffer (50 mM Tris, pH 7.4, 50 mM NaCl). The filters were equilibrated in scintillation vials containing 4 ml of UltimaGold scintillation fluid (PerkinElmer) and counted in a Packard Tricarb 2900TR Liquid Scintillation Analyzer (PerkinElmer). All data points were performed in duplicate or triplicate.

Western blot analysis. Frozen thymus, spleen, and brains from wt and PS2-deficient mice were rapidly homogenized in ice-cold homogenization buffer supplemented with Complete protease inhibitor mixture (Roche) (25 mM Tris-HCl, pH7.4, 50 mM NaCl, 0.5 mM EDTA), followed by 10 min centrifugation at 1000 *g*, +4°C. The postnuclear supernatant was subsequently centrifuged at 48,000 g for 30 min and the resultant pellet was resuspended in a low volume homogenization buffer and the protein content was determined using standard procedures (Pierce). Fifty micrograms of protein of each extract was solubilized in 2× SDS-PAGE loading buffer, heated to 37°C for 10 min and then electrophoresed in 4–12% NuPage mini-gels according to the manufacturer's instructions (Invitrogen). The gels were then subjected to electroblotting for 8 min (Invitrogen) to PDF membranes. After blocking the membranes in PBS containing 5% (w/v) milk and 0,05% (v/v) Tween 20, the membranes were incubated with anti-PS1 (Millipore Bioscience Research Reagents), anti-PS2 (Calbiochem), anti-Pen2 (UD-1), or anti-β-actin antibodies. When necessary, the membranes were stripped with protein stripping buffer between the antibody-membrane binding reactions. Each experiment

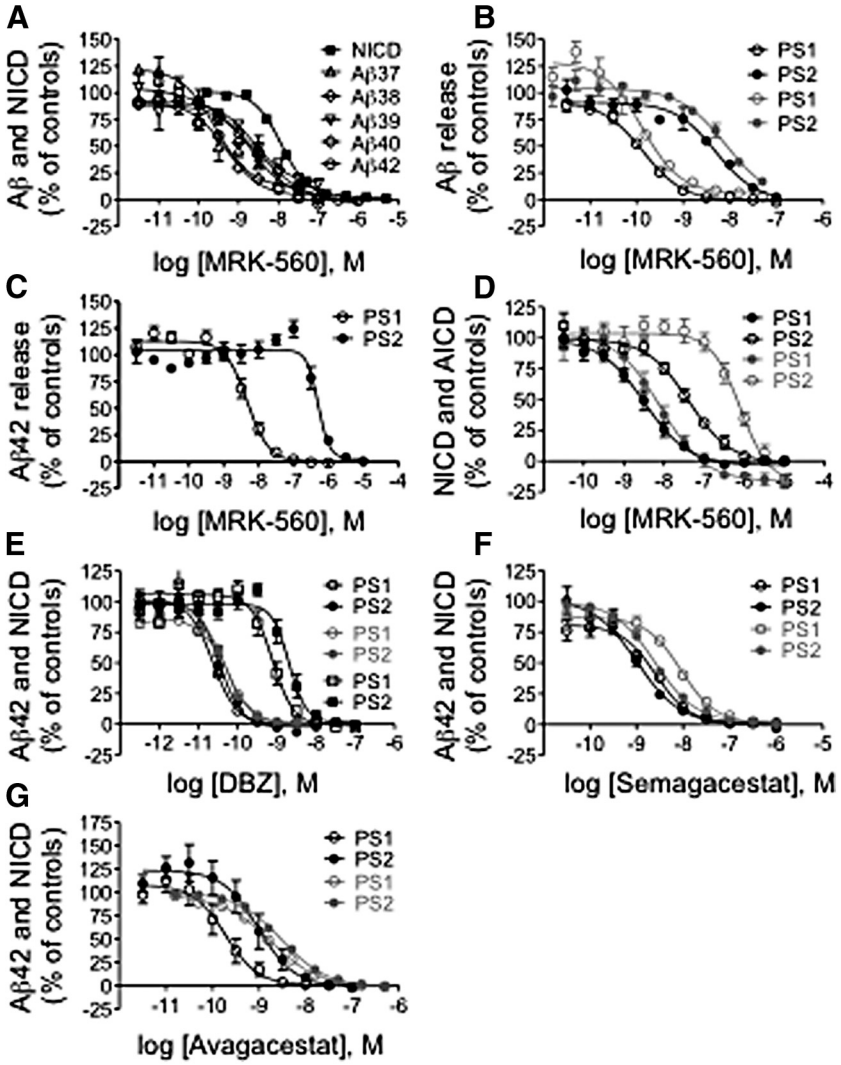

Figure 1. *In vitro* pharmacological profiling of MRK-560 and other GSIs. ***A***, MRK-560 inhibition of Aβ peptide generation and NICD translocation in HEK293 cells stably expressing APPswe and ΔENotch, respectively. ***B***, MRK-560 inhibition of Aβ42 and Aβ40 generation in HEK_PS1 and HEK_PS2 cells transiently transfected with C99 (black, Aβ42; gray, Aβ40). ***C***, MRK-560 inhibition of Aβ42 generation in BD8_PS1 and BD8_PS2 cells transiently transfected with C99. ***D***, MRK-560 inhibition of NICD and AICD in HEK_PS1 and HEK_PS2 cells (black, NICD; gray, AICD). ***E***, DBZ inhibition of Aβ42 peptide generation and NICD translocation in HEK293 cells stably expressing APPswe and ΔENotch and Aβ42 generation in BD8_PS1 and BD8_PS2 cells transiently transfected with C99 (squares, Aβ42(BD8)). ***F***, Semagecestat inhibition of Aβ42 generation and NICD translocation in HEK293 cells stably expressing APPswe and ΔENotch, respectively. ***G***, Avagecestat inhibition of Aβ42 generation and NICD translocation in HEK293 cells stably expressing APPswe and ΔENotch, respectively (black, Aβ42; gray, NICD in ***E–G***). The effect on Aβ42 production and NICD and AICD formation was analyzed after 5, 12, and 16 h, respectively, and plotted (mean ± SEM, $n = 3$, $n = 2$ for NICD and AICD, and $n = 1$ for Aβx-37, 38, and 39) relative to controls (0.5% DMSO and 0.5 μM L685458).

was finalized with horseradish peroxidase-conjugated secondary antibodies and antibody binding was monitored using chemiluminescence (Forte; Millipore) and standard x-ray films (Kodak).

RT-PCR analysis. Pieces of jejunum were dissected from C57BL/6 mice that had been treated with vehicle or MRK-560 (7.5 or 30 μmol/kg, once daily; see below) for 4 d. Total RNA was extracted and 1 μg of pure total RNA was primed with a mixture of poly-T and random oligonucleotides and reverse transcribed using Superscript II, according to standard protocols. The resulting reaction mixture was diluted 250 times and then aliquoted in a 96-well PCR plate for quantitative PCR. The cDNA was amplified using a 7500 Fast Real-Time PCR system using oligonucleotides specific for PS2 (5′-CTCAGCAAGCAAGCGTCTCTTC-3′ and 5′-TCCCAGCAGTCA CTGCAGAAAT-3′) and β-actin (5′-CACCCGCCACCAGTTCGC-3′ and 5′-GCACATGCCGGAGCCGTTGT-3′).

Animals and animal handling. Female 15-week-old WT C57BL/6 mice (Harlan Laboratories), male/female 18- to 30-week-old PS2-deficient mice (C57BL/6 background), and female 25-week-old Tg2576 mice (APP_{SWE} transgenic mice from Taconic) were used. Mice ($n = 6–10$) received vehicle alone, 7.5 or 30 μmol/kg MRK-560 subcutaneously (Tg2576: orally) once daily over 4 d in 20% hydroxypropyl-β-cyclodextrin (HPβCD) in 0.1 M Meglumin or 100 μmol/kg DBZ subcutaneously twice daily over 4 d in 0.5% HP methylcellulose (Methocel E4M)/0.1% Tween80 in water. Animals were anesthetized 3 h after the final dose and plasma was isolated from blood collected by cardiac puncture into EDTA tubes. Animals were killed by decapitation and brains were dissected into hemispheres for analysis of Aβ levels and drug concentration, whereas jejunum, thymus, and spleen were dissected for histopathological evaluation of Notch-related toxicity. It is of note that we did not detect any significant HPβCD-induced changes in basal Aβ levels as compared with nontreated or saline-treated mice. All animal experiments were performed in accordance with relevant guidelines and regulations provided by the Swedish Board of Agriculture. The ethical permission was provided by the Stockholm North Animal Research Ethical Board.

Measurement of drug and Aβ concentration in animal samples. Drug concentration in plasma and brain samples was determined by reversed-phase liquid chromatography and electrospray tandem mass spectrometry. Soluble Aβ was extracted from mouse brain tissue in diethylamine according to a standardized method (Borgegard et al., 2012). Aβ measurements were conducted by use of validated commercial ELISAs (BioSource and Innogenetics). All samples were analyzed in duplicate, and data analysis was performed using GraphPad Prism 4, one-way ANOVA followed by Dunnett's multiple-comparison test. Level of significance was set at $p \leq 0.05$.

Histopathological evaluation. At termination, spleen, thymus, and jejunum were dissected and placed in buffered formalin. After fixation, tissue samples were processed to wax blocks, sectioned, stained with hematoxylin and eosin (H&E), and examined by light microscopy. From each dose group, seven animals were used for histopathological evaluation. Histopathological changes were graded as follows: 0 = not present, 1 = minimal, 2 = slight, 3 = moderate, 4 = marked, 5 = severe. The scores were statistically analyzed using the nonparametric Kruskal–Wallis test, followed by Dunn's multiple-comparison test, as applied in the GraphPad Prism software. A p value of ≤ 0.05 was regarded as statistically significant.

Results

MRK-560 preferentially inhibits PS1-mediated processing of APP and Notch *in vitro*

The human cell line HEK293 expresses both PS1 and PS2. In these cells, we found that MRK-560 inhibited all Aβ species analyzed with similar potency, and displayed approximately sixfold selectivity for Aβ42 over NICD formation (Fig. 1*A*), which is in line with a previous report (Best et al., 2007). Next we addressed

whether γ-secretase complexes containing PS1 or PS2 were differentially sensitive to MRK-560. Overexpression of either PS1 or PS2 in HEK293 cells revealed that a much lower concentration of MRK-560 was sufficient to inhibit Aβ42 production in HEK293 cells expressing PS1 (IC_{50} = 0.144 nM), compared with cells expressing PS2 (IC_{50} = 5 nM), thus displaying >30-fold selectivity between PS1 and PS2, with similar potencies for Aβ40 (Fig. 1*B*). We also wanted to study if the PS1 selectivity would hold up also for the cleavage and release of APP intracellular domain (AICD). To assess this, we used a previously described luciferase reporter gene assay (Karlström et al., 2002). MRK-560 was shown to be an ~100-fold more potent inhibitor of PS1 compared with PS2-mediated AICD production (Fig. 1*D*). To address the PS specificity in a more defined genetic setting, we overexpressed PS1 or PS2 in mouse blastocyst-derived (BD8) cells lacking endogenous PS expression and thus γ-secretase activity (Donoviel et al., 1999; Strömberg et al., 2005). MRK-560 was shown to be a >100-fold more potent inhibitor of PS1 compared with PS2- mediated Aβ42 production (Fig. 1*C*). At low concentrations of MRK-560 an increase in the Aβ42 levels was detected (Fig. 1*C*). A transient increase in Aβ42 at low doses of GSI has been previously observed for various classes of GSIs, but the underpinning mechanism remains to be elucidated. We then tested whether the observed preference of MRK-560 for PS1 in APP processing also would be seen for Notch receptor processing. In HEK293 cells we expressed a truncated form of the Notch 1 receptor, Notch1ΔE, which is a membrane-tethered form of Notch that is independent of ligand activation but requires γ-secretase activity to generate an active NICD (Kopan et al., 1996). MRK-560 displayed a similar potency against PS1-mediated NICD formation (IC_{50} = 3 nM) as for AICD formation in PS1-expressing HEK293 cells (Fig. 1*D*). The IC_{50} value for MRK-560-mediated inhibition of PS2-catalyzed NICD formation was 42 nM[SCAP], i.e., ~13 times higher compared with PS1-expressing cells (Fig. 1*D*). We then explored the impact of PS subtype on the pharmacology of three GSIs representing different chemical classes: the DBZ, the benzolactam semagacestat (LY-450139), and the sulfonamide avagacestat (BMS-708163). These GSIs did not display an overt selectivity for either PS1- or PS2-mediated Aβ production, or NICD generation (Fig. 1*E–G*). Together, these data show that MRK-560, in contrast to several GSIs of different chemical classes that have been used in clinical trials, including the sulfonamide avagacestat, preferentially blocks PS1-mediated Aβ production and processing of Notch receptors. We also observed that less MRK-560 was required to displace [^{3}H]DBZ from membranes prepared from PS1-overexpressing cells compared with membranes from PS2 cells, suggesting that MRK-560 displays differential binding characteristics to PS1 and PS2 (Fig. 2*A*,*B*). The fact that MRK-560 did not completely displace [^{3}H]DBZ further supports a different mode of action between MRK-560 and DBZ. Furthermore, displacement binding studies of [^{3}H]DBZ to brain sections from PS2-deficient mice showed that MRK-560 could not completely displace [^{3}H]DBZ (Fig. 2*C–E*).

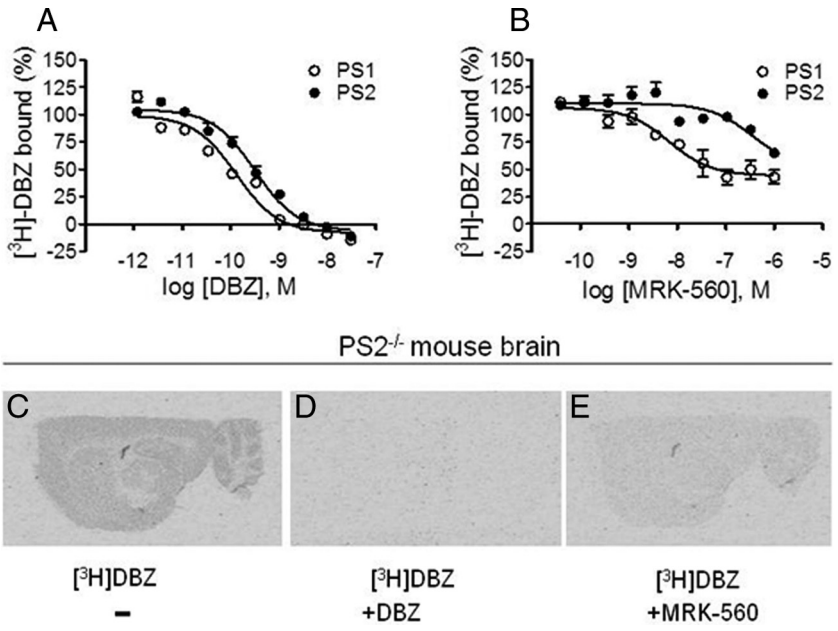

Figure 2. MRK-560 displays differential binding to PS1 and PS2. ***A***, ***B***, Displacement binding studies of [^{3}H]DBZ to membranes from HEK_PS1 and HEK_PS2 cells, respectively. DBZ (***A***) showed equipotent and full inhibition of [^{3}H]DBZ binding to both membrane preparations whereas MRK-560 (***B***) was more potent in displacing [^{3}H]DBZ from HEK_PS1 compared with HEK_PS2 membranes, but achieved only partial displacement of [^{3}H]DBZ. ***C–E***, Displacement binding studies of [^{3}H]DBZ to brain sections from PS2-deficient mice. ***C***, Total binding of 2 nM [^{3}H]DBZ. ***D***, Complete displacement of 2 nM [^{3}H]DBZ by 1 mM DBZ. ***E***, Partial displacement of 2 nM [^{3}H]DBZ by 1 mM MRK-560.

PS2 deficiency does not alter the distribution of MRK-560 in brain and plasma

The preference of MRK-560 for PS1-containing γ-secretase prompted us to explore whether the spared Notch signaling observed *in vivo* (Best et al., 2007) was a consequence of MRK-560 having an altered distribution in brain or plasma that precluded MRK-560 from reaching peripheral organs as efficiently as reaching the brain. To address this *in vivo*, WT and PS2-deficient mice were subjected to MRK-560 over 4 consecutive days and levels of MRK-560 were analyzed in plasma and brain 3 h after final administration. In both mouse genotypes, the concentration of MRK-560 was higher in plasma than in brain, and the level increased in a dose-dependent manner when the dose was elevated from 7.5 to 30 μmol/kg body weight (Table 1). An equal distribution profile was observed in WT and PS2-deficient mice, indicating that the distribution of MRK-560 between brain and plasma was not affected by the loss of PS2. The distribution profile of DBZ was, however, different between WT and PS2-deficient mice, with much higher concentration in the brains of PS2-deficient mice (Table 1).

MRK-560 potently reduces Aβ40 levels in WT and PS2-deficient mice

The effect of MRK-560 on Aβ40 levels in WT and PS2-deficient mice was next assessed. Mice received vehicle or MRK-560 at 7.5 or 30 μmol/kg body weight over 4 consecutive days. Measurement of Aβ40 levels in plasma and brain tissue samples 3 h after the final administration revealed a strong reduction in both plasma and brain Aβ40 levels in WT as well as PS2-deficient mice at the two doses tested (Fig. 3*A–D*). The observed twofold difference in plasma Aβ40 levels between WT and PS2-deficient mice receiving vehicle alone reflects an experimental variation in the baseline of endogenous plasma Aβ40 levels, but importantly, the reduction is of the same magnitude regardless of the baseline. Since it

Table 1. Exposure levels of MRK-560 and DBZ in plasma and brain of wild-type (A), PS2-deficient (B), and Tg2576 (C) mice 3 h after final dose on the fourth day

	Compound (Route)	Dose (μmol/kg)	C_p (nM)	$C_{br,\,corr}$ (nM)	$C_{u,p}$ (nM)	$C_{u,br,\,corr}$ (nM)
A	MRK-560 (s.c.)	7.5	3013	656	12	4
	MRK-560 (s.c.)	30	10843	2081	43	14
	DBZ (s.c.)	100	109	55	—	—
B	MRK-560 (s.c.)	7.5	3980	666	16	4
	MRK-560 (s.c.)	30	14690	3638	59	24
	DBZ (s.c.)	100	770	9291	—	—
C	MRK-560 (p.o.)	7.5	537	134	4	1
	MRK-560 (p.o.)	30	1494	531	6	4

C_p, Plasma concentration; $C_{br,\,corr}$, brain concentration corrected for plasma; $C_{u,\,p}$, free plasma concentration; $C_{u,\,br,\,corr}$, free brain concentration corrected for plasma.

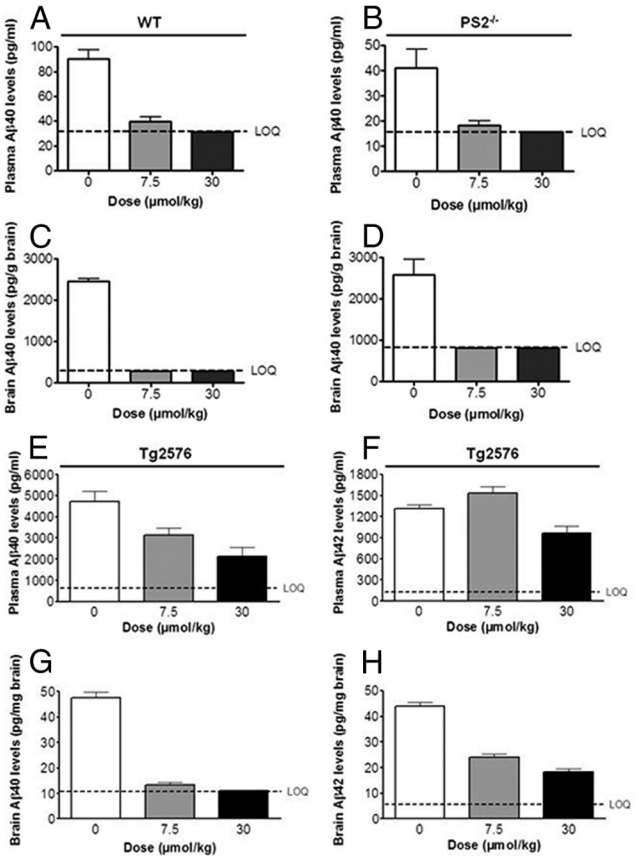

Figure 3. MRK-560 reduces Aβ40 and Aβ42 levels in plasma and brain. The levels of Aβ40 and Aβ42 were measured 3 h after the final administration of MRK-560 (7.5 and 30 μmol/kg) to WT (***A***, ***C***), PS2-deficient mice (***B***, ***D***), and Tg2576 mice (***E–H***). Data are presented as mean ± SEM with lower limit of quantification (LOQ) illustrated.

is difficult to detect endogenous Aβ42 in mice, mice overexpressing human APP (the Tg2576 strain, with readily detectable human Aβ42 levels) were also treated with vehicle or MRK-560 at 7.5 or 30 μmol/kg over 4 consecutive days. In Tg2576 mice, MRK-560 reduced both plasma and brain Aβ40 and Aβ42 levels (Fig. 3*E–H*), suggesting that MRK-560 is a bona fide GSI. Reduction in brain Aβ was, however, much more pronounced compared with the reduction of plasma Aβ (Fig. 3*E–H*). MRK-560 increased plasma levels of Aβ42 at the lower dose (Fig. 3*F*), in keeping with a previous report (Lanz et al., 2006).

The free plasma concentration of MRK-560 in WT and PS2-deficient mice (12 and 16 nM, respectively) at the 7.5 μmol/kg body weight dose (Table 1) exceeded the *in vitro* IC_{50} values for both PS1 and PS2 (0.144 and 5 nM, respectively), indicating that the concentration of inhibitor would be sufficient for an efficacious reduction of plasma Aβ40 in both WT and PS2-deficient mice. The measured free concentration of MRK-560 in WT and PS2-deficient mouse brains at the lower dose (4 nM) (Table 1) was in the same range as the *in vitro* IC_{50} for PS2, while it was much higher than the IC_{50} value for PS1-mediated Aβ production. Since the Aβ40 levels reached the lower limit of quantification (LOQ) in the brains of both WT and PS2-deficient mice, these data suggest that PS1 is the major enzyme of the brain catalyzing Aβ production, and reveal a good correlation between the *in vitro* pharmacology and free concentration of MRK-560 and its impact on Aβ levels in WT and PS2-deficient mice. The free concentration of MRK-560 in plasma and brain of Tg2576 mice after 4 d of oral administration (1–6 nM), was also in the same range as the *in vitro* IC_{50} for PS2 and higher than the IC_{50} value for PS1. The lower impact of MRK-560 on plasma compared with brain Aβ levels in these mice is consistent with the notion that PS2 contributes substantially to the plasma Aβ pool under conditions when PS1 is inactivated.

PS2-deficient, but not WT, mice exhibit Notch-related histopathology in response to MRK-560

We next examined whether MRK-560 caused a Notch-related histopathology in PS2-deficient mice. WT and PS2-deficient mice received 7.5 and 30 μmol/kg body weight MRK-560, and histological effects in organs known to be dependent on Notch signaling were analyzed (Searfoss et al., 2003). PS2-deficient mice developed Notch-related histopathological changes, i.e., goblet cell metaplasia in the jejunum, thymus atrophy, and reduction of the marginal zone in the spleen of some animals, after exposure to 7.5 (data not shown) and 30 μmol/kg MRK-560 (Fig. 4*C*,*F*,*I*). In contrast, WT mice treated with 30 μmol/kg MRK-560 showed no histological changes in the jejunum, thymus, or spleen (Fig. 4*B*,*E*,*H*) compared with vehicle controls (Fig. 4*A*,*D*,*G*). The difference in histopathological scores between PS2-deficient mice and WT controls was statistically significant for the jejunum and thymus, whereas the score for spleen did not reach statistical significance (Fig. 4*J–L*). Exposure to DBZ generated profound histopathological changes in both WT and PS2-deficient mice (Fig. 4*M–O*), in accordance with a previous report (Milano et al., 2004). In conclusion, these data show that PS2-deficient mice are sensitized to MRK-560 exposure, indicating an important role for PS2 in Notch processing in peripheral organs.

Impact of PS2 deficiency on γ-secretase expression levels and γ-secretase inhibitor binding in spleen, thymus, and brain

Since PS2 was important for Notch-dependent signaling in response to MRK-560, we wanted to learn whether PS2 deficiency impacted on the γ-secretase enzyme levels. First we analyzed by Western blot the levels of PS1, PS2, and the γ-secretase subunit Pen-2, which serves as a surrogate marker for mature γ-secretase enzymes. High levels of PS1 N-terminal fragment (NTF) were detected in all tissues from both WT and PS2-deficient mice. PS2 C-terminal fragment (CTF) was present in all tissues but expressed at a lower level compared with PS1 and only detected in tissues from WT mice (Fig. 5*A–C*). Whereas PS2 deficiency did not seem to affect PS1 NTF levels in any of the organs examined, the Pen-2 levels were not significantly altered in brain and thymus and spleen of PS2-deficient mice (Fig. 5*A–C*).

If PS2 would play a key role in Notch and APP processing in peripheral organs but not in the brain, it may be anticipated

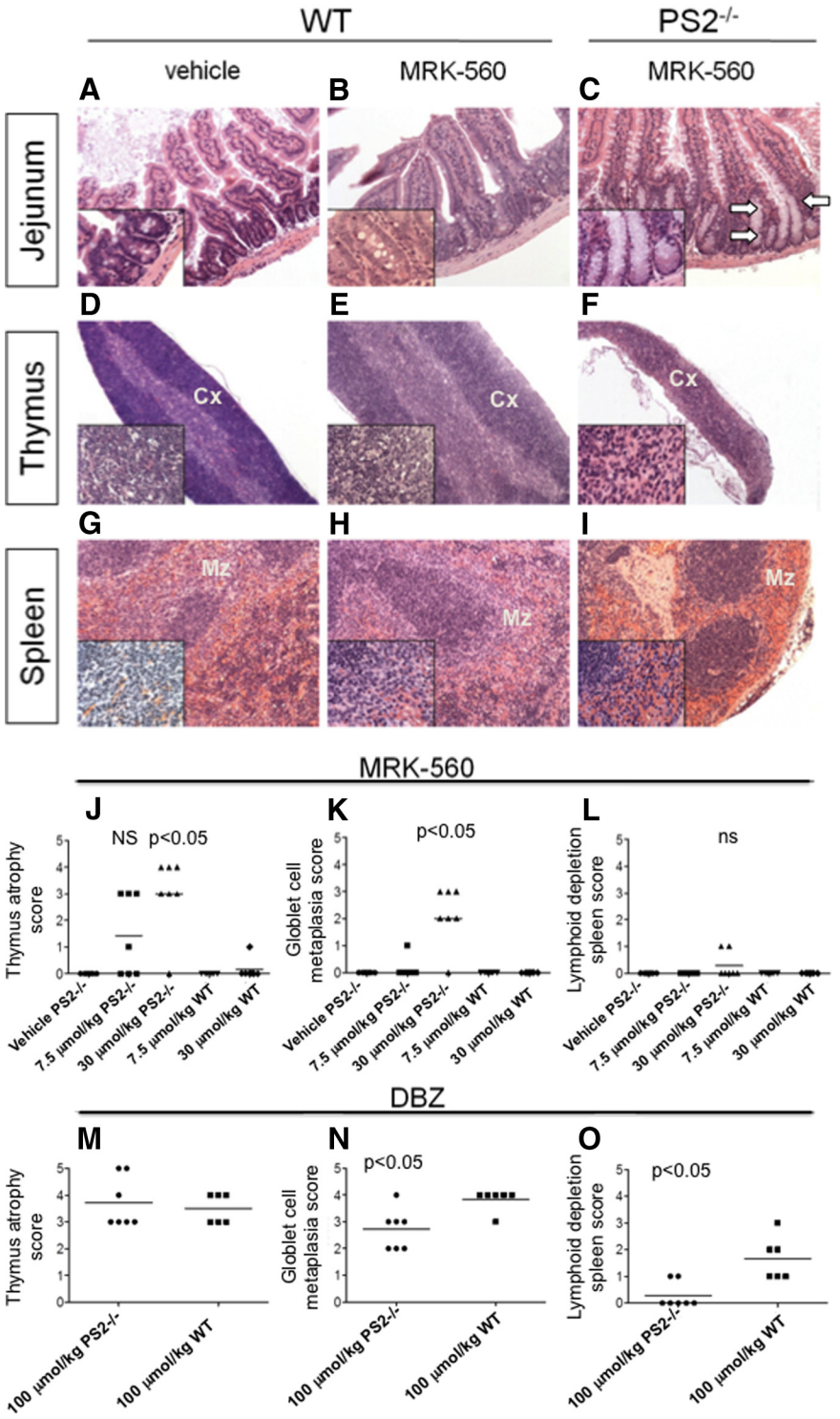

Figure 4. MRK-560 induces Notch-related histopathology in PS2-deficient mice**.** Histological sections from jejunum (***A–C***), thymus (***D–F***), and spleen (***G–I***) from WT (***A***, ***B***, ***D***, ***E***, ***G***, ***H***) and PS2-deficient (PS2$^{-/-}$) (***C***, ***F***, ***I***) mice. The mice were treated with MRK-560 at 30 μmol/kg (***B***, ***C***, ***E***, ***F***, ***H***, ***I***) or vehicle (***A***, ***D***, ***G***). PS2-deficient mice treated with MRK-560 showed goblet cell metaplasia (arrows) in the jejunum (***C***), atrophy of the thymic cortex (Cx) (***F***), and a reduction of the marginal zone (Mz) in the spleen (***I***). WT mice treated with MRK-560 (***B***, ***E***, ***H***) did not differ from vehicle-treated controls (***A***, ***D***, ***G***). H&E staining. Magnifications: 10× (***A–C***, ***G–I***), 4× (***D–F***), and inset in the lower left corner 40×. ***J–O***, Grading of Notch-related histopathology in mice treated with MRK-560 (***J–L***) and DBZ (***M–O***). The histopathological score (0–5) is shown on the *y*-axis, and the treatment group on the *x*-axis. *p* values refer to Dunn's multiple-comparison test. ***J***, ***M***, Thymus atrophy. ***K***, ***N***, Goblet cell metaplasia. ***L***, ***O***, Lymphoid depletion (marginal zone) in the spleen.

that PS2-deficient mice, compared with WT mice, would show reduced γ-secretase inhibitor binding in peripheral but not in brain tissue. To test this, we performed binding experiments with [^{3}H]DBZ on crude plasma membranes prepared from spleen, thymus, and brain from WT and PS2-deficient mice. We observed no significant difference in density of binding sites between WT and PS-deficient mice in any of the three tissues (Fig. 5*D–F*). These data suggest that removal of PS2 does not significantly alter the number of γ-secretase complexes and are in line with the Western blot data in Figure

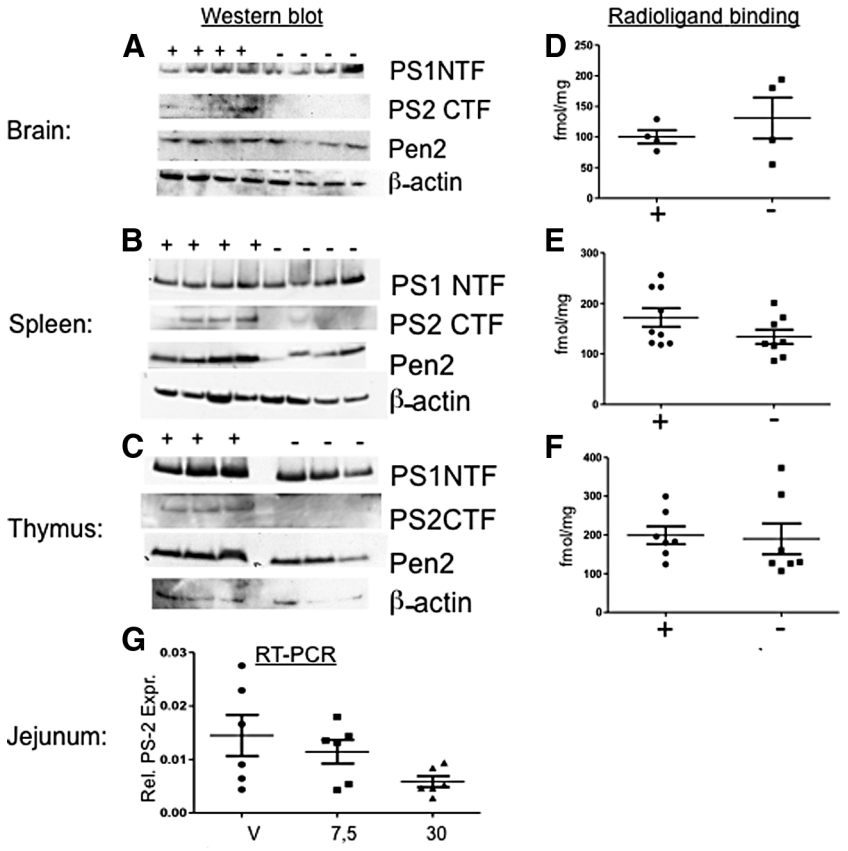

Figure 5. γ-Secretase expression in brain, thymus, and spleen of WT and PS2-deficient mice. ***A–C***, Western blot analysis of membrane extracts from brain (***A***), spleen (***B***), and thymus (***C***) from WT (+) and PS-deficient (−) mice revealed that PS1 and PS2 are expressed in all tissues examined (with the exception that PS2 is not expressed in PS2-deficient mice), and that PS1 is more highly expressed than PS2 in all three tissues. PS1 NTF, Presenilin 1 N-terminal fragment; PS2 CTF, Presenilin 2 C-terminal fragment; Pen-2, Presenilin enhancer 2. ***D–F***, Specific binding of 0.5 nM [^{3}H]DBZ in crude plasma membrane fraction from brain (***D***), spleen (***E***), and thymus (***F***) showed that binding was not significantly different when WT (+) was compared with PS2-deficient (−) tissue. Nonspecific binding was defined in the presence of 1 μM semagecestat. ***G***, RT-PCR analysis of PS2 and β-actin (housekeeping gene as control) mRNA levels in jejunum from C57BL/6 mice exposed to vehicle (V) or MRK-560 (7.5 μmol/kg and 30 μmol/kg, respectively) for 4 d. Each group represents six mice and the mean values of PS2 expression levels normalized to the β-actin expression levels are drawn in the graph.

5*A–C*, although it should also be noted that [^{3}H]DBZ may, in addition to γ-secretase, also bind to other enzymes such as PS homologs. To further assess whether PS2 compensates for PS1 function under conditions of PS1 inhibition, we tested whether the mRNA expression level of PS2 was altered by MRK-560. PS2 mRNA expression levels from jejunum prepared from WT mice or mice exposed to 7.5 or 30 μmol/kg MRK-560 for 4 d were not significantly different (Fig. 5*G*).

Collectively, the data are in accord with PS1 forming the majority of the γ-secretase in brain, spleen, and thymus, and that PS2 constitutes only a subset of the γ-secretase complexes in these tissues. The data, however, also indicate that PS2 can compensate for PS1 under conditions of PS1-specific inhibition, but that this is not a result of upregulation of PS2 levels.

Discussion

There is currently no disease-modifying therapy for AD, and to reduce Aβ production through γ-secretase inhibition is therefore a prioritized therapeutic approach. The outcome of clinical trials has thus far, however, been discouraging, which in most cases is likely due to Notch-related toxicity. Here we show that the preclinical GSI MRK-560 displays a high preference for PS1-containing γ-secretase activity, and causes Notch-related histopathology in mice lacking the PS2 gene at concentrations where WT mice are not affected. These findings, derived from genetic mouse models, suggest an important role for PS2 in regulating Notch signaling in the adult under conditions of PS1 inhibition and suggest PS2-sparing γ-secretase inhibition as a novel drug strategy for AD. In accord with this, clinical trials with PS2-sparing inhibitors have recently been initiated (Wu et al., 2012).

MRK-560 displayed similar potency with regard to APP and Notch processing but displayed specificity for PS1 over PS2 both with regard to APP and Notch processing. MRK-560 also showed a differential interaction to PS1 compared with PS2, providing a molecular explanation to the observed preference for PS1-containing γ-secretases. It has previously been proposed that GSIs of the sulfonamide type preferentially inhibit PS1-containing γ-secretase (Zhao et al., 2008; Borgegard et al., 2011), but our data show that the preference for PS1 versus PS2 processing varies considerably among different sulfonamide GSIs: MRK-560 exhibited a considerably stronger preference for PS1 over PS2 processing, whereas avagacestat (BMS-708163) did not. This difference is of interest with regard to the results from recent clinical trials, where avagacestat caused Notch-related side effects in Phase 2 clinical trials (Imbimbo et al., 2011). Similarly, the benzolactam semagacestat, which also failed in a clinical trial (Imbimbo et al., 2011), did not show a particular preference for PS subtype. It will therefore be worthwhile to explore whether GSIs with enhanced PS2 sparing, similar to MRK-560, would provide improved tolerability. In line with this, Lee et al, 2011, who recently reported similar findings on the preference for MRK-560 for PS1 secretases, described a compound with a 250-fold preference for PS1 over PS2, providing evidence of the feasibility of generating compounds with very high selectivity for PS1-mediated γ-secretase reactions.

MRK-560 caused a dose-dependent Notch-related toxicity only in the PS2-deficient mice, despite the fact that tissue penetration was similar in WT and PS2-deficient mice. The MRK-560-induced phenotypes observed in PS2-deficient mice, i.e., effects on jejunum, spleen, and thymus, are in good agreement with what has been observed by PS subtype nonspecific GSIs, such as DBZ (Fig. 4), and with data from genetic ablation of Notch signaling in these organs. Thus, cell type-specific ablation of Notch in the intestine leads to goblet cell metaplasia (van Es et al., 2005; Fre et al., 2005), and Notch is known to have key roles in various steps of T-cell development, which explains the phenotypes observed in spleen and thymus (Hadland et al., 2001; Radtke et al., 2004). While this

may in principle be explained by PS2 carrying out a major portion of Notch processing in the periphery, this seems less likely for several reasons. First, PS1 appears to be the predominant PS species not only in brain, but also in spleen and thymus. Second, the total amount of γ-secretase is not significantly reduced when PS2 is genetically ablated, as judged by Pen-2 expression or by the level of GSI binding on tissue sections. The fact that PS1-deficient mice display a severe embryonal phenotype in contrast to the relatively mild phenotype in PS2-deficient mice also supports an important role of PS1 in basal γ-secretase signaling in several peripheral tissues. It therefore appears reasonable to assume that PS2 can compensate for a sudden loss of PS1 activity caused, for example, by PS1-specific inhibition to an extent sufficient to avoid a dramatic phenotype. The fact that PS2 expression was not upregulated in response to MRK-560 treatment supports the notion that the PS2 compensation does not involve a dramatic transcriptional or translational upregulation, but may occur by, for example, post-translational modification or intracellular relocalization of the PS2 protein.

We also observed that MRK-560 was considerably more potent in lowering CNS Aβ levels compared with plasma Aβ levels in APP-overexpressing mice. These observations were made during conditions when drug exposure was similar in brain and plasma, and exceeded the *in vitro* determined IC_{50} value for PS1 and was in the same range as the IC_{50} value for PS2. These data are consistent with PS1 as a major generator of CNS Aβ production while PS2 appears to significantly contribute to the plasma Aβ pool, and are in good agreement with previously published data (Borgegard et al., 2011). It is noteworthy that higher doses of MRK-560 displayed a similar efficacy in lowering Aβ40 and 42 *in vivo* in APP-overexpressing (Tg2576) mice, but that at lower MRK-560 doses, plasma Aβ42 levels were increased compared with vehicle. The increase in plasma Aβ in the low-dose GSI range has been previously observed (Lanz et al., 2006) and is a potentially worrisome aspect of GSIs for future clinical use. Our data indicate that this feature of GSIs is retained in PS1-selective GSIs and needs to be carefully monitored in the further development of this class of drugs.

In conclusion, the data presented in this report shed new light on the mechanisms underpinning the PS1 specificity of certain sulfonamide GSIs and why a sulfonamide GSI with a strong preference for PS1 spares Notch signaling, thus avoiding unwanted Notch-related toxicity *in vivo*. Our data suggest that this mechanism of action may overcome some major limitations associated with the current GSIs that have failed in clinical testing, and indeed, very recently, Wu et al., 2012 reported on a PS1-selective inhibitor, SCH 900220, which has reached clinical trials. Future studies with this and other PS1-selective GSIs will eventually tell whether PS1-selective GSI is an efficacious and safe therapeutic strategy in AD.

References

Best JD, Smith DW, Reilly MA, O'Donnell R, Lewis HD, Ellis S, Wilkie N, Rosahl TW, Laroque PA, Boussiquet-Leroux C, Churcher I, Atack JR, Harrison T, Shearman MS (2007) The novel gamma secretase inhibitor N-[cis-4-[(4-chlorophenyl)sulfonyl]-4-(2,5-difluorophenyl)cyclohexyl]-1,1,1-trifluoromethanesulfonamide (MRK-560) reduces amyloid plaque deposition without evidence of notch-related pathology in the Tg2576 mouse. J Pharmacol Exp Ther 320:552–558. Medline

Borgegard T, Minidis A, Jureus A, Malmborg J, Rosqvist S, Gruber S, Almqvist H, Yan H, Bogstedt A, Olsson F, Dahlström J, Ray C, Närhi K, Malinowsky D, Hagström E, Jin S, Malmberg A, Lendahl U, Lundkvist J (2011) In vivo analysis using a Presenilin-1-specific inhibitor: presenilin1-containing γ-secretase complexes mediate the majority of CNS Aβ production in the mouse. Alzheimers Dis Res J 3:29–45.

Borgegard T, Juréus A, Olsson F, Rosqvist S, Sabirsh A, Rotticci D, Paulsen K, Klintenberg R, Yan H, Waldman M, Stromberg K, Nord J, Johansson J, Regner A, Parpal S, Malinowsky D, Radesater AC, Li T, Singh R, Eriksson H, et al. (2012) First and second generation gamma-secretase modulators (GSMs) modulate Abeta production through different mechanisms. J Biol Chem 287:11810–11819. CrossRef Medline

Churcher I, Beher D, Best JD, Castro JL, Clarke EE, Gentry A, Harrison T, Hitzel L, Kay E, Kerrad S, Lewis HD, Morentin-Gutierrez P, Mortishire-Smith R, Oakley PJ, Reilly M, Shaw DE, Shearman MS, Teall MR, Williams S, Wrigley JD (2006) 4-substituted cyclohexyl sulfones as potent, orally active gamma-secretase inhibitors. Bioorg Med Chem Lett 16:280–284. CrossRef Medline

De Strooper B, Saftig P, Craessaerts K, Vanderstichele H, Guhde G, Annaert W, Von Figura K, Van Leuven F (1998) Deficiency of presenilin-1 inhibits the normal cleavage of amyloid precursor protein. Nature 391:387–390. CrossRef Medline

De Strooper B, Annaert W, Cupers P, Saftig P, Craessaerts K, Mumm JS, Schroeter EH, Schrijvers V, Wolfe MS, Ray WJ, Goate A, Kopan R (1999) A presenilin-1-dependent gamma-secretase-like protease mediates release of Notch intracellular domain. Nature 398:518–522. CrossRef Medline

Donoviel DB, Hadjantonakis AK, Ikeda M, Zheng H, Hyslop PS, Bernstein A (1999) Mice lacking both presenilin genes exhibit early embryonic patterning defects. Genes Dev 13:2801–2810. CrossRef Medline

Fre S, Huyghe M, Mourikis P, Robine S, Louvard D, Artavanis-Tsakonas S (2005) Notch signals control the fate of immature progenitor cells in the intestine. Nature 435:964–968. CrossRef Medline

Haapasalo A, Kovacs DM (2011) The many substrates of presenilin/γ-secretase. J Alzheimers Dis 25:3–28. Medline

Hadland BK, Manley NR, Su D, Longmore GD, Moore CL, Wolfe MS, Schroeter EH, Kopan R (2001) Gamma-secretase inhibitors repress thymocyte development. Proc Natl Acad Sci U S A 98:7487–7491. CrossRef Medline

Imbimbo BP, Panza F, Frisardi V, Solfrizzi V, D'Onofrio G, Logroscino G, Seripa D, Pilotto A (2011) Therapeutic intervention for Alzheimer's disease with γ-secretase inhibitors: still a viable option? Expert Opin Investig Drugs 20:325–341. CrossRef Medline

Karlström H, Bergman A, Lendahl U, Näslund J, Lundkvist J (2002) A sensitive and quantitative assay for measuring cleavage of presenilin substrates. J Biol Chem 277:6763–6766. CrossRef Medline

Karran E, Mercken M, De Strooper B (2011) The amyloid cascade hypothesis for Alzheimer's disease: an appraisal for the development of therapeutics. Nat Rev Drug Discov 10:698–712. CrossRef Medline

Kopan R, Schroeter EH, Weintraub H, Nye JS (1996) Signal transduction by activated mNotch: importance of proteolytic processing and its regulation by the extracellular domain. Proc Natl Acad Sci U S A 93:1683–1688. CrossRef Medline

Lanz TA, Karmilowicz MJ, Wood KM, Pozdnyakov N, Du P, Piotrowski MA, Brown TM, Nolan CE, Richter KE, Finley JE, Fei Q, Ebbinghaus CF, Chen YL, Spracklin DK, Tate B, Geoghegan KF, Lau LF, Auperin DD, Schachter JB (2006) Concentration-dependent modulation of amyloid-beta in vivo and in vitro using the gamma-secretase inhibitor, LY-450139. J Pharmacol Exp Ther 319:924–933. CrossRef Medline

Lee J, Song L, Terracina G, Bara T, Josien H, Asberom T, Sasikumar TK, Burnett DA, Clader J, Parker EM, Zhang L (2011) Identification of presenilin 1-selective γ-secretase inhibitors with reconstituted γ-secretase complexes. Biochemistry 50:4973–4980. CrossRef Medline

Malmquist J, Bernlind A, Sandell J, Ström P, Waldman M (2012) Tritium labeling of two γ-secretase inhibitors and one modulator as *in vitro* imaging agents. J Label Compd Radiopharm 55:80–83. CrossRef

Milano J, McKay J, Dagenais C, Foster-Brown L, Pognan F, Gadient R, Jacobs RT, Zacco A, Greenberg B, Ciaccio PJ (2004) Modulation of notch processing by gamma-secretase inhibitors causes intestinal goblet cell metaplasia and induction of genes known to specify gut secretory lineage differentiation. Toxicol Sci 82:341–358. CrossRef Medline

Morohashi Y, Kan T, Tominari Y, Fuwa H, Okamura Y, Watanabe N, Sato C, Natsugari H, Fukuyama T, Iwatsubo T, Tomita T (2006) C-terminal fragment of presenilin is the molecular target of a dipeptidic gamma-secretase-specific inhibitor DAPT (N-[N-(3,5-difluorophenacetyl)-L-

alanyl]-S-phenylglycine t-butyl ester). J Biol Chem 281:14670–14676. CrossRef Medline

Radtke F, Wilson A, Mancini SJ, MacDonald HR (2004) Notch regulation of lymphocyte development and function. Nat Immunol 5:247–253. CrossRef Medline

Saura CA, Choi SY, Beglopoulos V, Malkani S, Zhang D, Shankaranarayana Rao BS, Chattarji S, Kelleher RJ 3rd, Kandel ER, Duff K, Kirkwood A, Shen J (2004) Loss of presenilin function causes impairments of memory and synaptic plasticity followed by age-dependent neurodegeneration. Neuron 42:23–36. CrossRef Medline

Searfoss GH, Jordan WH, Calligaro DO, Galbreath EJ, Schirtzinger LM, Berridge BR, Gao H, Higgins MA, May PC, Ryan TP (2003) Adipsin, a biomarker of gastrointestinal toxicity mediated by a functional gamma-secretase inhibitor. J Biol Chem 278:46107–46116. CrossRef Medline

Serneels L, Dejaegere T, Craessaerts K, Horré K, Jorissen E, Tousseyn T, Hébert S, Coolen M, Martens G, Zwijsen A, Annaert W, Hartmann D, De Strooper B (2005) Differential contribution of the three Aph1 genes to gamma-secretase activity in vivo. Proc Natl Acad Sci U S A 102:1719–1724. CrossRef Medline

Serneels L, Van Biervliet J, Craessaerts K, Dejaegere T, Horré K, Van Houtvin T, Esselmann H, Paul S, Schäfer MK, Berezovska O, Hyman BT, Sprangers B, Sciot R, Moons L, Jucker M, Yang Z, May PC, Karran E, Wiltfang J, D'Hooge R, et al. (2009) gamma-Secretase heterogeneity in the Aph1 subunit: relevance for Alzheimer's disease. Science 324:639–642. CrossRef Medline

Steiner H, Fluhrer R, Haass C (2008) Intramembrane proteolysis by gamma-secretase. J Biol Chem 283:29627–29631. CrossRef Medline

Strömberg K, Hansson EM, Laudon H, Bergstedt S, Näslund J, Lundkvist J, Lendahl U (2005) gamma-Secretase complexes containing N- and C-terminal fragments of different presenilin origin retain normal gamma-secretase activity. J Neurochem 95:880–890. CrossRef Medline

van Es JH, van Gijn ME, Riccio O, van den Born M, Vooijs M, Begthel H, Cozijnsen M, Robine S, Winton DJ, Radtke F, Clevers H (2005) Notch/gamma-secretase inhibition turns proliferative cells in intestinal crypts and adenomas into goblet cells. Nature 435:959–963. CrossRef Medline

Wu W-L, Domalski M, Burnett DA, Josien H, Bara T, Rajagopalan M, Xu R, Clader J, Greenlee WJ, Brunskill A, Hyde LA, Del Vecchio RA, Cohen-Williams ME, Song L, Lee J, Terracina G, Zhang Q, Nomeir A, Parker EM, Zhang L (2012) Discovery of SCH 900229, a potent presenilin 1 selective γ-secretase inhibitor for the treatment of Alzheimer's Disease. ACS Med Chem Lett 3:892–896. CrossRef

Zhao B, Yu M, Neitzel M, Marugg J, Jagodzinski J, Lee M, Hu K, Schenk D, Yednock T, Basi G (2008) J Biol Chem 283:2927–2938. Medline